Desalination and Water Treatment
www.deswater.com

doi: 10.1080/19443994.2015.1137235

57 (2016) 23505–23515
October

Taylor & Francis
Taylor & Francis Group

High antibiofouling property of vertically aligned carbon nanotube membranes at a low cross-flow velocity operation in different bacterial solutions

Kwang-Jin Lee, Eunji Cha, Hee-Deung Park*

School of Civil, Environmental and Architectural Engineering, Korea University, Anam-Dong, Seongbuk-Gu, Seoul 136-713, South Korea, Tel. +82 2 3290 4861; Fax: +82 2 928 7656; emails: illdo4u@daum.net (K.-J. Lee), toto7608@gmail.com (E. Cha), heedeung@korea.ac.kr (H.-D. Park)

Received 30 September 2015; Accepted 26 December 2015

ABSTRACT

While membranes have been widely applied in water and wastewater treatment, further studies are still needed on the fouling issues. Vertically aligned carbon nanotube (VA CNT), an antibacterial nanomaterial, is a promising candidate for a membrane because of its superfast water permeability. The antibacterial and antibiofouling properties of VA CNT membranes were reported with a high permeate flux. This study showed the high antibiofouling property of VA CNT membranes at low cross-flow velocity operation in different bacterial solutions, resulting from its high antibacterial property, along with a quantitative comprehension of the relation between biofilms and fouling resistance of VA CNT membranes after membrane operation. These results facilitated the possibility of using VA CNT membranes for wastewater treatment, such as membrane bioreactors, even at a very low cross-flow velocity.

Keywords: Antibacterial; Biofouling; Carbon nanotube; Membrane; Vertically aligned

1. Introduction

Although the use of membranes is a promising technology in water and wastewater treatment processes, membrane fouling is an issue that still needs to be understood and mitigated. Membrane fouling is divided into four categories according to the species of foulants: particulate, organic, inorganic, and biofouling [1]. Biofouling is defined as the unwanted deposition and growth of biofilms [2], and is regarded as "the Achilles heel" of membrane processes [3]. Biofilm is composed of the aggregates of cells, extra polymeric substance (EPS), and other particulate matter that accumulated on the surfaces [4]. Biofilm development on membrane surface results in many problems, including a decrease in the membrane permeate flux (by increasing fouling layer resistance and concentration polarization) and hindrance of crossflow on the membrane surface [5]. However, until now, after more than 30 years of studies on biofouling, it has not been clearly understood [6].

Carbon nanotubes (CNTs) are reported to possess superfast water transport through their inner pores, and have chemical-resistance, adsorption, and antibiofouling properties [7]. These are attractive features for fabricating membranes. It has been hypothesized that the toxicity of CNTs could be applied to reduce

*Corresponding author.

biofouling [8]. CNTs are reported to mechanically damage bacterial cell membranes [9] and they were applicable to both Gram-negative and -positive bacteria [10]. In addition, CNTs are sparingly dispersed in water (i.e. low wettability) due to their superhydrophobic property [11], which reduces cell viability [12]. Commercial membranes have been composited with CNTs to prevent biofouling [8], but the compatibilities between CNTs and membranes still need to be solved. To enhance the adhesion strength of CNTs on the membrane surface, the covalent binding of single-walled (SW) CNTs to RO membranes increased the long-term antimicrobial property [13]. A synergistic effect of nanosilver particles and multi-walled (MW) CNTs was reported to decrease the biofouling of the microfiltration (MF) membrane [14]. However, they also showed two limitations. One was the leaching problem because of weak adhesion and the other was a lower flux than the original membrane because of the decreased porosity.

The vertically aligned (VA) CNT membranes using inner holes as membrane pores showed ultra-high water permeability [15], and after reinforcement their leachate did not show any antibacterial effect [16]. Several studies have previously reported that VA CNT membranes mitigate permeate water flux declination [17,18]. Thus, the next logical step would be to more quantitatively study the antibiofouling properties of VA CNT membranes, especially concerning certain aspects of their biofilm and membrane performance.

Many studies concerning biofouling on membranes [19] also correlated biofilm analysis with quantitative techniques, such as optical density at 545 nm (OD_{545}), confocal laser scanning microscopy (CLSM) and Fourier-transform infrared (FT-IR) at an attenuated total reflectance (ATR) mode, and fouling resistance to evaluate membrane biofouling [20]. The early study on membrane biofilms in an RO membrane, using live/dead cell analysis [21], showed that as the permeate water flux decreased, the biofilms matured more rapidly during membrane operation, and the biofilms dominated the dead bacteria. The traditional quantification of biofilm was to observe the absorbance of extracted crystal violet-stained biofilm. The microbial strains and their biofilms on the substrate surface can be characterized by FT-IR spectroscopy at an ATR mode [22] in real time. One study used CLSM [23] to three-dimensionally observe the biofilm formed by single-strain bacteria.

Concerning the aspects of the membrane, bacterial fouling on the membrane has on occasion been compared with the classical pore blocking model, such as colloidal fouling [24], but most studies have related membrane biofouling to biofilm. Biofilm has been reported to be closely dependent on fouling resistance [25]. In a resistance in series model [26], membrane fouling resistance was determined by the difference between the membrane and total resistances calculated from the measured permeate fluxes of the pristine and fouled membranes. Biofouling on membranes is very important and should be quantitatively analyzed in terms of biofilms and also for fouling resistance. While the VA CNT membranes can show very good antibiofouling property during their operation, they have seldom been studied. This property can reduce the cross-flow velocity that consumes much of the energy of the pressurized membrane operation in a membrane bioreactor. Choi et al. [27] showed that the formation of a reversible fouling layer was prevented by a cross-flow velocity of 2.0 m/s for an ultrafiltration (UF) membrane. However, their biofouling study was limited to biofilms by a single strain. Another study [28] showed the impacts of SW CNTs on the microbial community structure in activated sludge (AS), but there were no results for a dynamic state, such as membrane operation.

The main purpose of this study was to show the high antibiofouling property of VA CNT membranes at a low cross-flow velocity operation in different bacterial solutions, resulting from its high antibacterial property, along with a quantitative comprehension of the relation between biofilms and the fouling resistance of VA CNTs during and after membrane operation. First, single strains representing Gram-negative and -positive bacteria was used for a more quantitative understanding of the antibacterial property of the VA CNT membrane; AS was then used for a more practical understanding to show the possibility of application to a membrane bioreactor even at a low cross-flow velocity. The commercial UF membranes of similar pore size as VA CNT membranes were adapted to all the same experiments as the control.

2. Materials and methods

2.1. VA CNT synthesis and VA CNT membrane fabrication

The VA CNT synthesis and VA CNT membrane fabrication procedures followed the protocols of a previous study [16]. The VA CNT synthesis was based on the water vapor assisted chemical vapor deposition (CVD) process. The VA CNTs were grown on an Fe (1.5 nm)/Al (15 nm)/Si wafer. After the coating, the Si wafer was cut into rectangular chips with the dimensions of 9 mm width and 9 mm length, and the cut chips were inserted into a cylindrical electric

furnace of a CVD machine. The carbon source was high-purity ethylene gas (99.99%) and its flow rate was 100 standard cubic centimeters per minute, indicating cc/min at a standard temperature and pressure (sccm). The carrier gas was argon (99.999%) and its flow rate was 300 sccm. Hydrogen gas (200 sccm; 99.999%) and water vapor (50 sccm) by argon purging were added to the gases stream. The reaction was carried out at 750˚C for 40 min.

The interstitial space between the synthesized VA CNTs was filled using a CRP 7005B urethane monomer (T&L, Yongin, Korea) ethanol solution at a 3:7 volume ratio in a mold. Ethanol was used as a densification agent and as an inducer for urethane monomer, filling the interstitial space between the CNTs. After infiltration, a CRP 7005B monomer was cross-linked in the interstitial space of the CNTs at 40˚C for 12 h. After the cross-linking, the top and bottom of the CNT membranes were cut by a microtome to open the CNT's caps and the membrane edges were extended by additional cross-linking by a different urethane monomer (UC-40 A, B, Cytec, Yongin, Korea) which was of a higher hardness to fit the membrane operation test unit and provide high pressure durability.

2.2. Bacterial solution preparation

Pseudomonas aeruginosa PA14 (PA14) and *Staphylococcus aureus* strain ATCC6538 (SA) were used as Gram-negative and -positive model bacteria, respectively. After overnight culture of each bacterium on Luria–Bertani (LB) agar plates, a single colony was inoculated in 60 ml of LB broth (10 g/L tryptone, 5 g/L yeast extract, 10 g/L NaCl). The bacterial strain was cultured in an incubator at a shaking rate of 250 rpm at 37˚C for 12 h. When the growth of the cultured bacterial solutions reached the late exponential phase, they were diluted with 6 L of fresh synthetic wastewater medium (1:100, v/v). The synthetic wastewater was prepared, following the protocol set by Herzberg and Elimelech [21]: the synthetic wastewater was composed of 1.16 mM trisodium citrate dihydrate, 0.94 mM ammonium chloride, 0.45 mM KH_2PO_4, 0.50 mM $CaCl_2{\cdot}2H_2O$, 0.50 mM $NaHCO_3$, 2.0 mM NaCl, and 0.60 mM $MgSO_4{\cdot}7H_2O$. An optical density value at 595 nm (OD_{595}) of diluted bacterial solution was confirmed to be 0.010, as read by a UV–vis spectrophotometer (DR 5000, Hach, Loveland, USA). The AS of the aeration tank was sampled at the Kiheung Wastewater Treatment Plant (Yongin, Korea) and it was used in the membrane fouling test without any dilution. Its mixed-liquor suspended solids concentration was 3,000 mg/L.

2.3. Membrane operation—biofouling

A VA CNT membrane and a commercial UF membrane (UE4040, Toray Chemical, Kumi, Korea), having a similar pore size as a control, were tested at 25˚C using a membrane test unit (Fig. 1). Prior to the membrane biofouling operation, the testing membrane was compacted with 6 L of deionized (DI) water at 4 bar transmembrane pressure (TMP) and a 10 cm/s cross-flow velocity (L_v) for 3 h. After membrane compaction, synthetic wastewater was added to the DI water following 2 h of equilibrium time. A bacterial solution was subsequently added and the permeate water flux was monitored. When AS was used for the biofouling test, the DI water was drained after membrane compaction, and 6 L of AS was added to the feed tank without the addition of synthetic wastewater. During the membrane operation, the growth of each bacterium was monitored every 2 h by OD_{595} in influent water. The inflow, permeate flow, temperature of source water, and TMP were automatically monitored. The bacterial solution was stirred to protect against aggregation or precipitation (MSH-20A, Wisestir, WisdLab Instruments, Wertheim, Germany) and air was supplied by an air generator through a Teflon filter (0.22 μm) during the biofouling test. The size of the UF membrane cell was 5.5 cm × 5.5 cm × 0.25 cm (width × length × height), and that of the VA CNT membrane was 0.2 cm × 0.2 cm × 0.01 cm. All permeate and concentrate water were returned to the feed tank. The biofouling was in operation for 36 h.

The test unit was cleaned at the end of the biofouling test. The sequence was as follows. 0.5% (v/v) NaOCl was circulated for 3 h to disinfect and oxidize organic matters. After the NaOCl was drained, tap

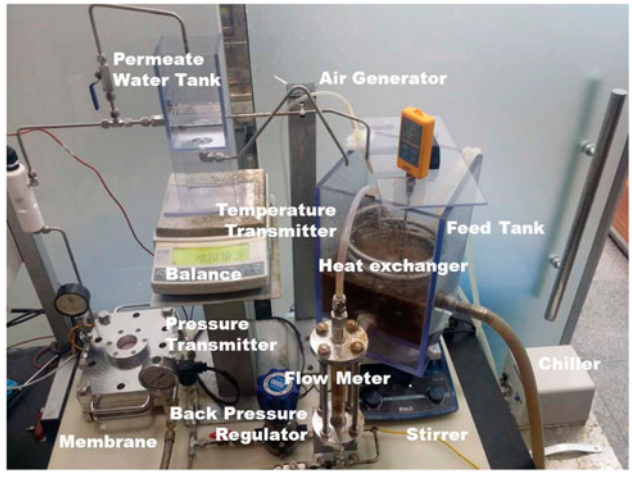

Fig. 1. Biofouling test unit used in this study.

water was circulated for 10 min, twice. After tap water flushing, 1% (m/v) oxalic acid was circulated for 6 h. For the final flushing, tap water and DI water were subsequently circulated for 10 min three times. During the cleaning, the flow rate was 1 L/min.

2.4. Quantification of biofilms

Biofilm causing biofouling of membranes was quantitatively analyzed using two methods and visually checked by CLSM. After the membrane operation, fouling resistance and OD_{545} were used for biofilm quantification, and Concanavalin A (Con A)-stained biofilm was optically compared with the other two results.

2.4.1. Fouling resistance

The fouling resistance (the summation of reversible and irreversible fouling resistance) was calculated by the difference between total resistance and membrane resistance in Eq. (1) as follows:

$$R_{tot} = R_m + R_r + R_{ir} \quad (1)$$

where R_{tot} is total resistance, R_m is membrane resistance, R_r is reversible fouling resistance, and R_{ir} is irreversible fouling resistance.

Membrane resistance was calculated from the water permeability achieved in the graph of TMP vs. flux as the slope of their linear dependence before the fouling test, using the following Eq. (2):

$$J = \frac{\Delta P}{u \times R} \text{ or } R = \frac{1}{u \times \frac{J}{\Delta P}} = \frac{1}{u \times L_p} \quad (2)$$

where J is the permeate water flux, ΔP is the TMP (bar), u is the viscosity of water (Pa s), R is the resistance (m^{-1}), and L_p is the water permeability (L/m^2 h bar).

The tested fluxes were calculated from TMPs at 2.0, 2.5, 3.0, 3.5, and 4.0 bar. Eq. (2) is available when the TMP and water temperature are constant during the membrane operation. Total resistance was calculated in the same way as membrane resistance, but was achieved after the fouling test was finished. The fouling resistance was calculated from the difference between the total and membrane resistance.

2.4.2. CLSM

After the biofouling test, a quarter of the tested membrane surface was washed twice with phosphate-buffered saline (PBS) (Sigma Aldrich, St. Louis, USA). The membrane surface was stained with 200 μL of Con A (Sigma Aldrich) for 30 min in the dark at room temperature. The Con A stains carbohydrate in EPS was detected by phosphorescence. After washing twice with PBS, the CLSM (Zeiss LSM 700, Jena, Germany) images of the stained membrane were taken with a lens of W N-Achroplan 20×/0.5 W (DIC) M27. The total magnification was 200×. All the images had the same threshold value.

2.4.3. Crystal violet

After the biofouling test, half of the tested membrane was rinsed twice with PBS. The membrane was stained with 0.1% crystal violet for 30 min and soaked in DI water to remove the residual crystal violet for 1 h in the shaker (SLOS-1D, MyLab, Seoul, Korea). The crystal violet (stained biofilm on a membrane surface) was extracted using 50 mL of 99.9% ethanol (Sigma Aldrich) in the sonicator (WiseClean, Wisd Laboratory Instruments, Wertheim, Germany) for 10 min at 30˚C at 30% power. The OD_{545} value of the extracted crystal violet ethanol solution was measured and subtracted from the value of the pristine membrane following the same procedure as the control. All the OD_{545} values were normalized by a membrane area of 10 cm^2.

2.5. Antibacterial property

The antibacterial property of each membrane was tested following the protocols of Lee and Park [16] using L7012 LIVE/DEAD *Bac*Light Bacterial Viability Kits (Invitrogen, Carlsbad, USA). In comparing the growth rate of each bacterium to determine whether or not they were directly exposed to the VA CNT membrane surface, the antibacterial property of the VA CNT membrane for the bacterial solution was analyzed. After the biofouling test, a quarter of the membrane was stained and analyzed by CLSM. The SYTO 9 (3 μL) and PI (3 μL) were used to stain the nucleic acid of the bacteria for 15 min in the dark at room temperature. The CLSM images were taken using the same procedure as the biofilm analysis with Con A. It showed the antibacterial property of the VA CNT membrane to bacteria on the membrane surface.

3. Results and discussion

3.1. VA CNT synthesis and VA CNT membrane fabrication

The VA CNT forest was grown by the CVD and densified in a mold. The densification of VA CNTs

and cross-linking of urethane were carried out on a Si wafer substrate, and the densified VA CNTs were removed from the substrate. Former studies [29–31] also showed the densification procedure of the VA CNT forest by capillary forces [32] with a volatile solvent. However, the reinforcer filling procedures in the narrow interstitial space between the VA CNTs (with large size fillers such as parylene [33], epoxy [29], and polystyrene) were less efficient. In this study, ethanol could effectively deliver a small CRP 7005B urethane monomer into the interstitial space. The densification was critically maximized by the pressing of mold walls. The encased edge of the VA CNT membrane was covered by polytetrafluoroethylene tape for installation to a membrane test unit. The dimension of the VA CNT was 80 mm in width and 80 mm in length, and after the densification, it was reduced to 2.45 mm in width and 2.75 mm in length. The average effective area of the CNT forest was 64.1 mm^2, whereas that of the densified CNT was 6.7 mm^2, thus it was densified by 960%.

3.2. Permeate water flux

Fig. 2 shows the flux (J/J_0) decline over time for the VA CNT and UF membranes (Table 1) operated with the feed solutions of PA14, SA, and AS for 36 h. The cross-flow (linear) velocity (10 cm/s) was 10 to 20 times lower than the common side-stream MBR operation (100–200 cm/s) [27]. The UF membrane showed dramatic permeate flux decline for all the feed solutions. The operational times to reach half of the initial flux were 5.4, 1.9, and 0.24 h for PA14, SA, and AS solutions, respectively. The UF membrane was fully fouled by the AS solution within a short period of time (<30 min) compared with the PA14 or SA solution. After 36 h of operation, the flux was less than 5% of the initial flux for all the feed solutions. However, the VA CNT membrane was resistant to biofouling compared with the UF membrane. The final J/J_0 values were 0.72, 0.59, and 0.40 for the PA14, SA, and AS solutions, respectively. This result demonstrated the possibility of low cross-flow velocity operation using the VA CNT membrane, which could be a key factor to overcome the high energy consumption issue of pressurized membrane modules in a membrane bioreactor process.

The fast permeate flux decline by the SA or PA14 solution from 0 to 15 h of operation time appears to have a close relationship to their bacterial growth (Fig. 3). This period was overlapped with the exponential growth phase of the bacteria. Biofilm was formed from 10 h [21] at the same operational condition. Up to 10 h, the bacterial deposition is presumed to dominate the membrane fouling (i.e. due to the increased concentration of bacteria resulting from the growth). The SA showed a higher growth rate and higher flux decline in this period than PA14 (Fig. 3), which is in agreement with the faster flux decline by SA solution than by PA14 solution.

3.3. Antibacterial property

During the membrane fouling operation, the bacterial growth was monitored every 2 h as OD_{595}. Fig. 3 shows the growth curves of SA and PA14, respectively. The 10 cm/s of cross-flow velocity corresponded to 1 L/min of cross-flow. For 36 h of the biofouling test because the test unit was a closed system where all water in the feed tank was fully returned, the single-strain bacteria or cells, in the AS in 6 L of feed tank, had a total of 360 chances to make direct contact with the membrane surface (= 1 L/min × 1 cycle/6 L × 36 h × 60 min/h). The growth or morphology of all bacterial cells monitored by OD_{595} could be affected by the contact with the membrane surface during the biofouling test. All bacteria showed a lower maximum of OD_{595}, longer growth time than the batch growth test, and a slight decline of OD_{595} after the exponential growth phase because of the poor nutrients supply and low temperature [21], even though there was enough aeration. The SA showed higher maximum OD_{595} values than PA14, but a similar ending time of exponential growth, cor-

Table 1
Membrane specification used in this study

Membrane properties	VA CNT membrane	UF membrane
Average inner diameter (nm)	4.1	5.7
Wall number of CNTs	4–5	–
Thickness (μm)	1,000	20
Pore density (10^{10} pore/cm^2)	300	9
Effective membrane area (cm^2)	0.453	38.4
Sealing material	Polyurethane	Polysulfone

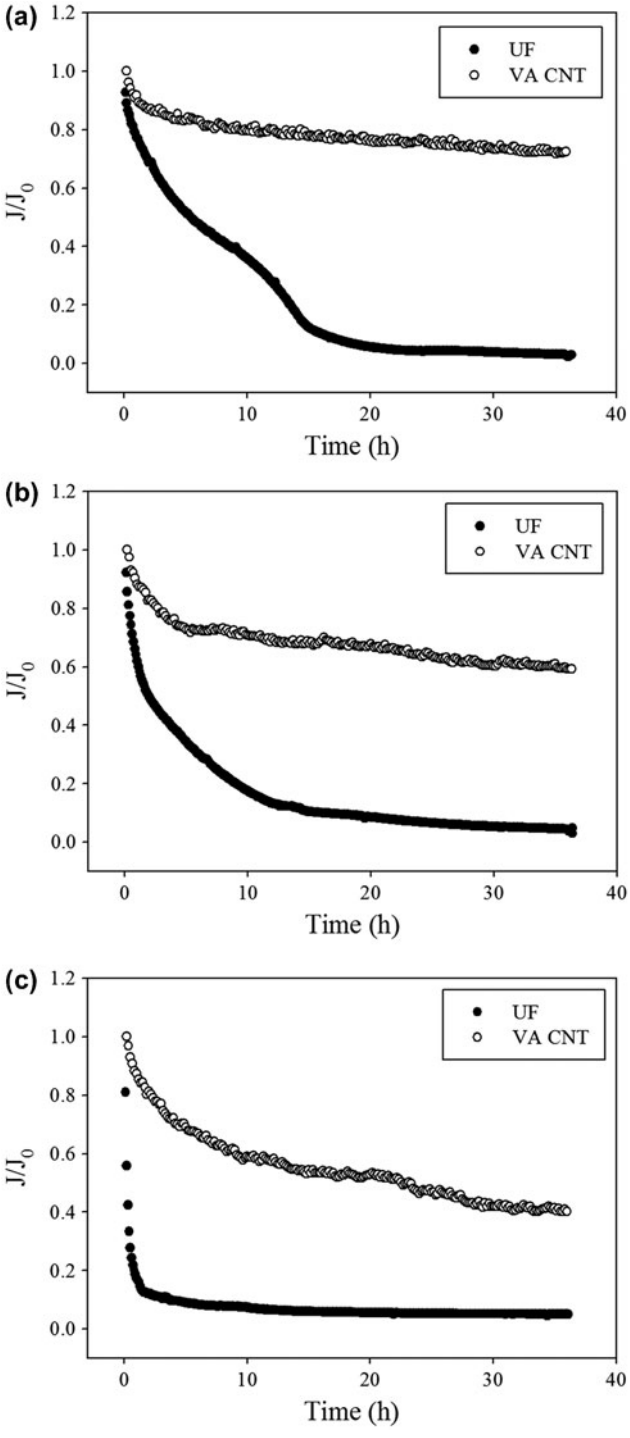

Fig. 2. Flux (J/J_0) decline over time for the VA CNT membrane and the UF membrane operated with the feed solutions of PA14 (a), SA (b), and AS (c).

responding to its batch growth test. The most important result was that the VA CNT membrane did not show any antibacterial property to planktonic PA14

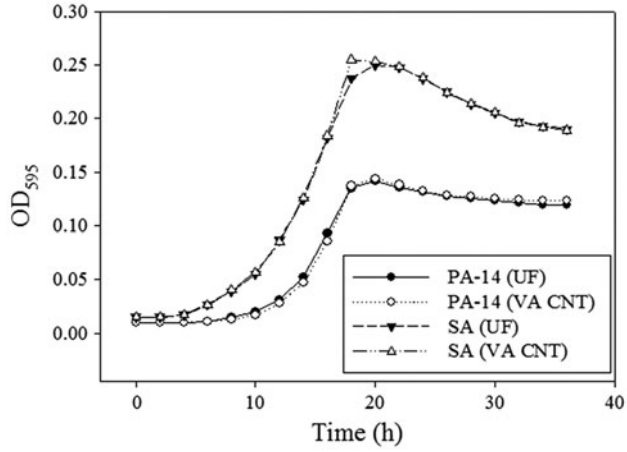

Fig. 3. Growth of PA14 and SA in feed water tank during the operation of the biofouling test unit equipped with UF or VA CNT membrane.

and SA, representing Gram-negative and -positive bacteria, respectively, in the bacterial feed solution, which agrees with a previous study [16].

Fig. 4 shows the live (green) and dead (red) cells in different colors. Fig. 4(a), (c), and (e) show the bacteria (PA14 (a), SA (c), AS (e)) on biofouled VA CNT membrane surfaces after the operation, while Fig. 4(b), (d), and (f) show cells (PA14 (b), SA (d), AS (f)) on biofouled UF membrane surfaces. At the end of the operation, there were as many dead bacteria as live bacteria on all six-fouled membranes, which was as expected from the growth results demonstrating the OD_{595} (Fig. 3). Similar results were found in the result of Herzberg and Elimelech [21]. However, the total density of cells on the VA CNT membranes was much smaller than that on the UF membranes (see VA CNT and UF membranes before and after the biofouling test in Supplementary Figures). This resulted from the difference in the adhesion strength of the cells exposed to the membrane surfaces, even though all fouled membranes were washed by the same procedure before the staining, by means of changing the morphologies of the cells from direct contact [9]. Similar to the results of a previous study [16], this study showed the antibacterial property of the CNT membrane surfaces after direct contact. However, this study showed a higher density of PA14 and higher density of dead PA14, because we did not flush the cells on the membrane surfaces before the staining, and the dead PA14 and weak adhesive PA14 were easily flushed out. Nevertheless, both studies showed the same result, that is, a high antibacterial property of the VA CNT membrane surface. In comparison with the difference of the cells, the residual cell

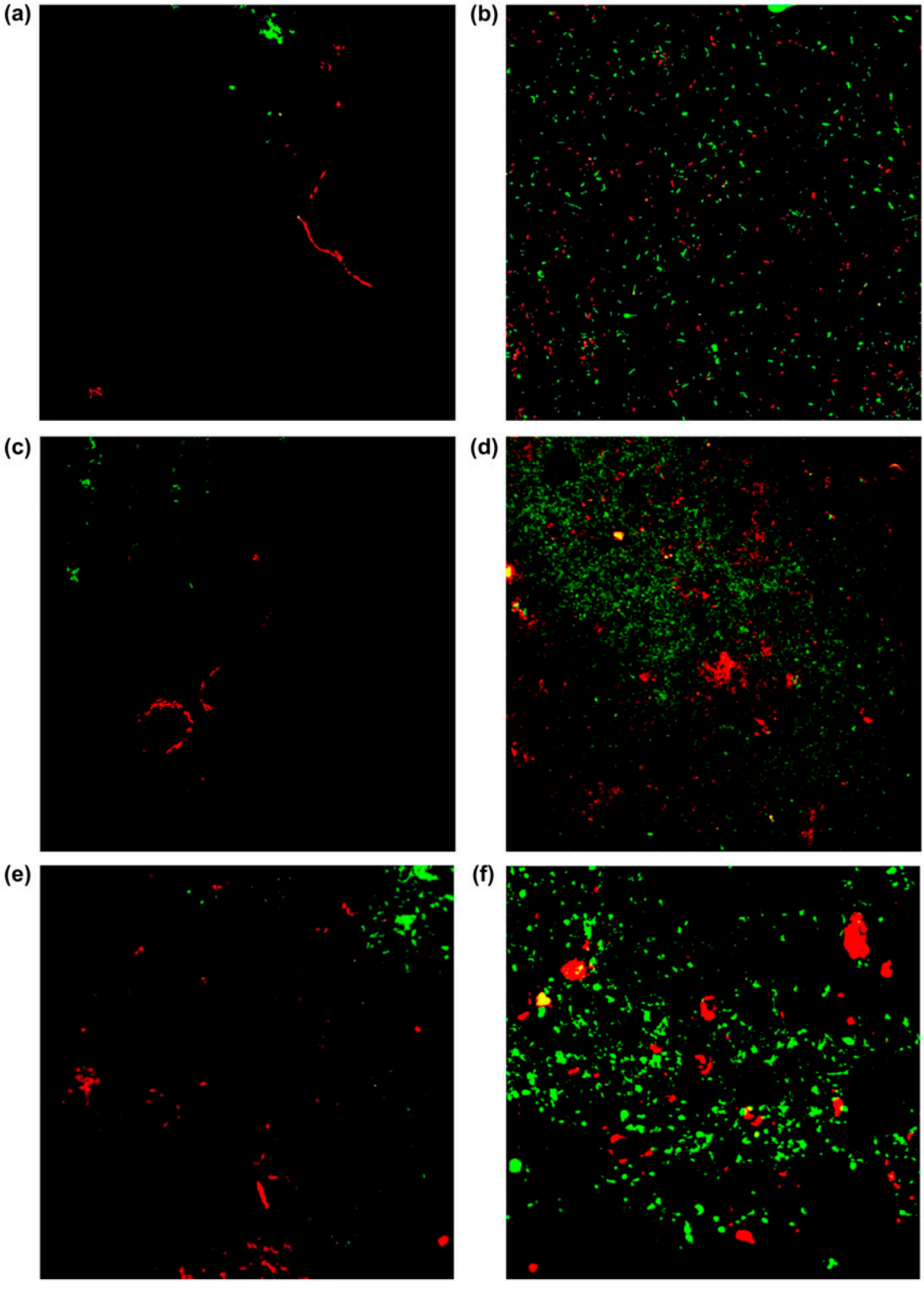

Fig. 4. Live/dead cell analysis results: PA14 on the fouled VA CNT (a) and UF (b) membrane surfaces. SA on the fouled VA CNT (c) and UF (d) membrane surfaces. AS on the fouled VA CNT (e) and UF (f) membrane surfaces.

numbers on the fouled membrane surfaces were proportional to the concentration of feed water.

3.4. Biofilm analysis

Biofilm, mainly causing biofouling, was analyzed using three methods. One method involved fouling resistance, as calculated from the difference between the total and membrane resistances. Fig. 5 shows the fouling resistances (R_{fs}) of the UF and VA CNT membranes fouled by PA14, SA, and AS solutions. The R_{fs} of VA CNT membranes fouled by PA14, SA, and AS solutions were 2.0, 3.0, and $7.0 \times 10^{10}\ m^{-1}$, respectively. They were 1,000–3,000 times smaller than those of the UF membranes fouled by the three types of solutions. The reduced number of bacteria formed fewer fouling layers because of the antibacterial damage on the VA CNT membrane surfaces. The order of the antibacterial damage was AS > SA > PA14 (Fig. 4), which resulted in the same order of R_f. The antibacterial damages on the membrane surfaces could mitigate biofilm, therefore, reduced biofouling.

This order trend was similar to the OD_{545} of the extracted crystal violet result from the stained biofilm on the fouled membrane. Fig. 6 shows the OD_{545} results of the UF and VA CNT membranes fouled by the PA14, SA, and AS solutions. The OD_{545} values were all zero for biofilms on the surface of the VA CNT membranes fouled by PA14, SA, and AS solutions. After being flushed with the DI water before staining, almost no cells remained on the VA CNT membrane surface after the fouling test. Furthermore, small amounts of bacteria or their biofilms existed on the VA CNT membrane surfaces fouled by the PA14 and SA solutions, immediately after the fouling test was finished. In the case of the UF membrane fouling,

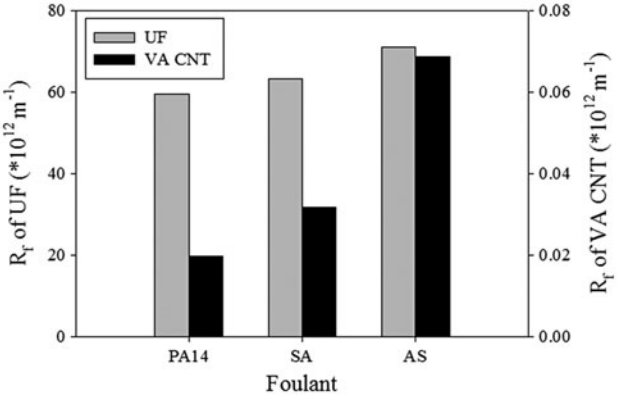

Fig. 5. Fouling resistances of UF and VA CNT membranes fouled by PA14, SA, and AS.

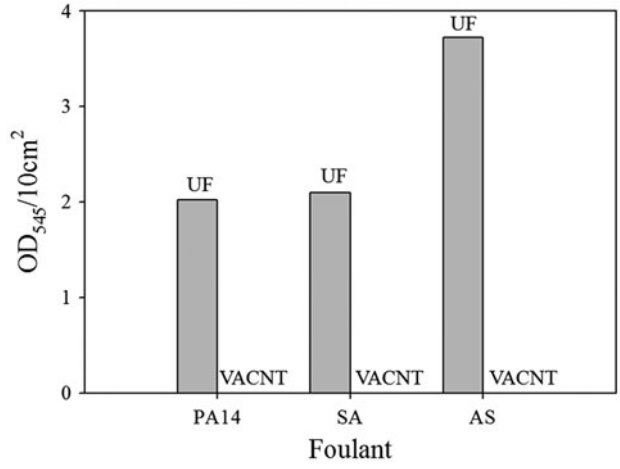

Fig. 6. OD_{545} results of the UF and VA CNT membranes fouled by PA14, SA, and AS.

the order of OD_{545} was the same as that of R_f, but the OD_{545} of biofouled UF membranes was 1.8 times higher than the other values, and this difference differed significantly from the result of R_f. It is likely that a low density biofilm was formed by the AS.

The order trend of OD_{545} representing the amount of total biofilm was proportional to the intensity of the ConA signal in the CLSM images (Fig. 7), thereby representing the amount of carbohydrates consisting of biofilm. All the ConA-stained biofilms on the UF membranes showed a higher density than that on the VA CNT membranes; furthermore, the ConA-stained biofilms on the UF membrane, fouled by the PA14, SA, and AS solutions, showed thicknesses of 10, 35, and 80 μm, respectively. The overwhelmingly thickest biofilm formed by AS on UF membrane coincided with the OD_{545} of the UF membrane. The trend of the ConA-stained biofilms on the VA CNT membranes fouled by PA14, SA, and AS was the same as the result of the R_{fs}.

3.5. Mechanistic explanation of antibiofouling property in VA CNT membrane

This study showed that the single strain of bacteria or cells in AS were damaged on the surfaces of the VA CNT membranes during the membrane operation, as also shown in a previous study on the antibacterial property of the CNT-based membrane [16], even though there were two obvious differences: the existence of the membrane permeation and the system volume. Various studies [34–40] have reported antimicrobial properties of suspended CNTs, showing overall damages to planktonic bacteria. However, those studies showed different results, whereby the

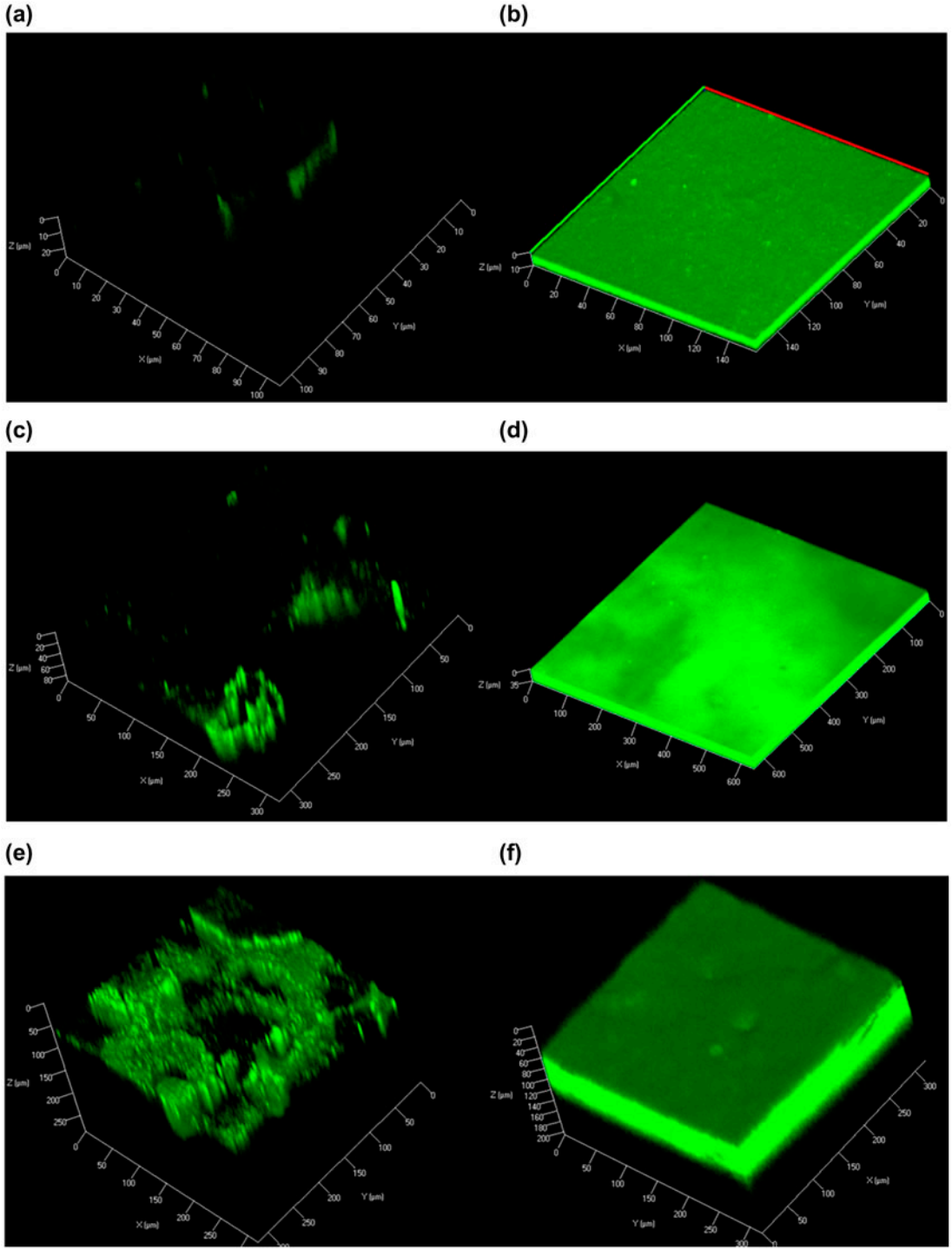

Fig. 7. ConA-stained biofilms analyzed by CLSM: PA14 on the fouled VA CNT (a) and UF (b) membrane surfaces. SA on the fouled VA CNT (c) and UF (d) membrane surfaces. AS on the fouled VA CNT (e) and UF (f) membrane surfaces.

integrated VA CNT did not show any damage to the bacterial growth and only showed an antibacterial property against the bacteria on their surfaces. The suggested mechanisms of the antibacterial properties of CNTs are mechanical piercing such as "nano-darts" [41], electrochemical damages [42], and toxicity of the catalysts embedded in the CNTs [35]. All mechanisms were closely related to the direct and continuous

contact between the CNTs and bacteria. A higher number of dead cells (higher ratio of red to green color) were observed on the CNT membranes than on the UF membranes (see Fig. 4).

Because of the long fouling test time (36 h) with insufficient nutrients, all the surfaces of the membranes showed many dead cells (red colored cells in Fig. 4). However, the VA CNT membranes reduced the number of bacterial cells on their surfaces after 36 h of the fouling test. This could result from the combination of the ultrahigh hydrophobicity and weakened adhesion between the bacteria or cells and the membrane surfaces. Finally, this decrease in the number of bacteria or cells resulted in a dramatically low density of biofilm on the VA CNT membrane surfaces after the fouling test.

Taken together, this study suggests that there could be a synergistic effect, combined with the ultrahigh hydrophobicity and an antibacterial property, on the decrease in cell number on VA CNT membranes during the operation, on the decrease in biofilm density, and on the decrease in the biofouling on the VA CNT membrane surfaces.

4. Conclusions

The VA CNT membranes showed an antibacterial property only on their surfaces during the operation, which concurs with the static antibacterial result of a previous study [16]. The bacterial growth was not inhibited by the VA CNT membranes during the long period of direct exposure. This localized antibacterial property of VA CNT membranes dramatically reduced the biofilm on the membrane surface. The VA CNT membranes showed the possibility of operating at a low cross-flow velocity because of their high antibiofouling property, which could not be achieved with a commercial membrane. It is a promising result for pressurized membrane modules in membrane bioreactors, which have shown high energy consumption for high cross-flow velocity against biofouling. To the best of our knowledge, it was the first study to show the possibility of the VA CNT membranes for wastewater treatment, such as membrane bioreactors, even at a very low cross-flow velocity.

Supplementary material

The supplementary material for this paper is available online at http://dx.doi.10.1080/19443994.2015.1137235.

Acknowledgments

This study was supported by the Basic Science Research Program through the National Research Foundation of Korea funded by the Ministry of Education, Science and Technology (NRF-2012M3A7B4049863).

References

[1] W. Guo, H.-H. Ngo, J. Li, A mini-review on membrane fouling, Bioresour. Technol. 122 (2012) 27–34.
[2] H.-C. Flemming, Biofouling in water systems–cases, causes and countermeasures, Appl. Microbiol. Biotechnol. 59 (2002) 629–640.
[3] H.C. Flemming, G. Schaule, T. Griebe, J. Schmitt, A. Tamachkiarowa, Biofouling—The Achilles heel of membrane processes, Desalination 113 (1997) 215–225.
[4] Z. Lewandowski, H. Beyenal, Biofilms: Their structure, activity, and effect on membrane filtration, Water Sci. Technol. 51 (2005) 181–192.
[5] J. Gutman, S. Fox, J. Gilron, Interactions between biofilms and NF/RO flux and their implications for control—A review of recent developments, J. Membr. Sci. 421–422 (2012) 1–7.
[6] R. Komlenic, Rethinking the causes of membrane biofouling, Filtr. Sep. 47 (2010) 26–28.
[7] K.-J. Lee, H.-D. Park, The most densified vertically-aligned carbon nanotube membranes and their normalized water permeability and high pressure durability, J. Membr. Sci. 501 (2016) 144–151.
[8] V.K. Upadhyayula, V. Gadhamshetty, Appreciating the role of carbon nanotube composites in preventing biofouling and promoting biofilms on material surfaces in environmental engineering: A review, Biotechnol. Adv. 28 (2010) 802–816.
[9] S. Kang, M. Herzberg, D.F. Rodrigues, M. Elimelech, Antibacterial effects of carbon nanotubes: Size does matter! Langmuir 24 (2008) 6409–6413.
[10] S. Liu, A.K. Ng, R. Xu, J. Wei, C.M. Tan, Y. Yang, Y. Chen, Antibacterial action of dispersed single-walled carbon nanotubes on *Escherichia coli* and *Bacillus subtilis* investigated by atomic force microscopy, Nanoscale 2 (2010) 2744–2750.
[11] H. Zanin, C.M. Rosa, N. Eliaz, P.W. May, F.R. Marciano, A.O. Lobo, Assisted deposition of nano-hydroxyapatite onto exfoliated carbon nanotube oxide scaffolds, Nanoscale 7 (2015) 10218–10232.
[12] H. Zanin, L. Hollanda, H. Ceragioli, M. Ferreira, D. Machado, M. Lancellotti, R. Catharino, V. Baranauskas, A. Lobo, Carbon nanoparticles for gene transfection in eukaryotic cell lines, Mater. Sci. Eng. C 39 (2014) 359–370.
[13] A. Tiraferri, C.D. Vecitis, M. Elimelech, Covalent binding of single-walled carbon nanotubes to polyamide membranes for antimicrobial surface properties, ACS Appl. Mater. Interfaces 3 (2011) 2869–2877.
[14] E.S. Kim, G. Hwang, M.G. El-Din, Y. Liu, Development of nanosilver and multi-walled carbon nanotubes thin-film nanocomposite membrane for enhanced water treatment, J. Membr. Sci. 394–395 (2012) 37–48.

[15] J.K. Holt, H.G. Park, Y. Wang, M. Stadermann, A.B. Artyukhin, C.P. Grigoropoulos, A. Noy, O. Bakajin, Fast mass transport through sub-2-nanometer carbon nanotubes, Science 312 (2006) 1034–1037.
[16] K.-J. Lee, H.-D. Park, The effect of morphologies of carbon nanotube-based membranes and their leachates on antibacterial property, Desalin. Water Treat. doi: 10.1080/19443994.19442015.11025585.
[17] S.-M. Park, J. Jung, S. Lee, Y. Baek, J. Yoon, D.K. Seo, Y.H. Kim, Fouling and rejection behavior of carbon nanotube membranes, Desalination 343 (2014) 180–186.
[18] B. Lee, Y. Baek, M. Lee, D.H. Jeong, H.H. Lee, J. Yoon, Y.H. Kim, A carbon nanotube wall membrane for water treatment, Nature Commun. 6 (2015), doi: 10.1038/ncomms8109.
[19] S.T. Kang, A. Subramani, E.M.V. Hoek, M.A. Deshusses, M.R. Matsumoto, Direct observation of biofouling in cross-flow microfiltration: Mechanisms of deposition and release, J. Membr. Sci. 244 (2004) 151–165.
[20] W. Lee, C.H. Ahn, S. Hong, S. Kim, S. Lee, Y. Baek, J. Yoon, Evaluation of surface properties of reverse osmosis membranes on the initial biofouling stages under no filtration condition, J. Membr. Sci. 351 (2010) 112–122.
[21] M. Herzberg, M. Elimelech, Physiology and genetic traits of reverse osmosis membrane biofilms: A case study with *Pseudomonas aeruginosa*, ISME J. 2 (2008) 180–194.
[22] J. Schmitt, H.-C. Flemming, FTIR-spectroscopy in microbial and material analysis, Int. Biodeterior. Biodegrad. 41 (1998) 1–11.
[23] M. Klausen, A. Heydorn, P. Ragas, L. Lambertsen, A. Aaes-Jørgensen, S. Molin, T. Tolker-Nielsen, Biofilm formation by *Pseudomonas aeruginosa* wild type, flagella and type IV pili mutants, Mol. Microbiol. 48 (2003) 1511–1524.
[24] S. Chellam, N.G. Cogan, Colloidal and bacterial fouling during constant flux microfiltration: Comparison of classical blocking laws with a unified model combining pore blocking and EPS secretion, J. Membr. Sci. 382 (2011) 148–157.
[25] R. McDonogh, G. Schaule, H.C. Flemming, The permeability of biofouling layers on membranes, J. Membr. Sci. 87 (1994) 199–217.
[26] L. Defrance, M. Jaffrin, Reversibility of fouling formed in activated sludge filtration, J. Membr. Sci. 157 (1999) 73–84.
[27] H. Choi, K. Zhang, D.D. Dionysiou, D.B. Oerther, G.A. Sorial, Influence of cross-flow velocity on membrane performance during filtration of biological suspension, J. Membr. Sci. 248 (2005) 189–199.
[28] D. Goyal, X. Zhang, J. Rooney-Varga, Impacts of single-walled carbon nanotubes on microbial community structure in activated sludge, Lett. Appl. Microbiol. 51 (2010) 428–435.
[29] Y. Baek, C. Kim, D.K. Seo, T. Kim, J.S. Lee, Y.H. Kim, K.H. Ahn, S.S. Bae, S.C. Lee, J. Lim, High performance and antifouling vertically aligned carbon nanotube membrane for water purification, J. Membr. Sci. 460 (2014) 171–177.
[30] F. Du, L. Qu, Z. Xia, L. Feng, L. Dai, Membranes of vertically aligned superlong carbon nanotubes, Langmuir 27 (2011) 8437–8443.
[31] M. Yu, H.H. Funke, J.L. Falconer, R.D. Noble, High density, vertically-aligned carbon nanotube membranes, Nano Lett. 9 (2008) 225–229.
[32] D.N. Futaba, K. Hata, T. Yamada, T. Hiraoka, Y. Hayamizu, Y. Kakudate, O. Tanaike, H. Hatori, M. Yumura, S. Iijima, Shape-engineerable and highly densely packed single-walled carbon nanotubes and their application as super-capacitor electrodes, Nat. Mater. 5 (2006) 987–994.
[33] P. Krishnakumar, P. Tiwari, S. Staples, T. Luo, Y. Darici, J. He, S. Lindsay, Mass transport through vertically aligned large diameter MWCNTs embedded in parylene, Nanotechnology 23 (2012) 455101.
[34] S. Kang, M. Pinault, L.D. Pfefferle, M. Elimelech, Single-walled carbon nanotubes exhibit strong antimicrobial activity, Langmuir 23 (2007) 8670–8673.
[35] S. Kang, M.S. Mauter, M. Elimelech, Microbial cytotoxicity of carbon-based nanomaterials: Implications for river water and wastewater effluent, Environ. Sci. Technol. 43 (2009) 2648–2653.
[36] A.L. Alpatova, W. Shan, P. Babica, B.L. Upham, A.R. Rogensues, S.J. Masten, E. Drown, A.K. Mohanty, E.C. Alocilja, V.V. Tarabara, Single-walled carbon nanotubes dispersed in aqueous media via non-covalent functionalization: Effect of dispersant on the stability, cytotoxicity, and epigenetic toxicity of nanotube suspensions, Water Res. 44 (2010) 505–520.
[37] C.P. Firme III, P.R. Bandaru, Toxicity issues in the application of carbon nanotubes to biological systems, Nanomedicine 6 (2010) 12.
[38] C. Yang, J. Mamouni, Y. Tang, L. Yang, Antimicrobial activity of single-walled carbon nanotubes: Length effect, Langmuir 26 (2010) 16013–16019.
[39] Y. Bai, I.S. Park, S.J. Lee, T.S. Bae, F. Watari, M. Uo, M.H. Lee, Aqueous dispersion of surfactant-modified multiwalled carbon nanotubes and their application as an antibacterial agent, Carbon 49 (2011) 3663–3671.
[40] L. Dong, A. Henderson, C. Field, Antimicrobial activity of single-walled carbon nanotubes suspended in different surfactants, J. Nanotechnol. 2012 (2011).
[41] S. Liu, L. Wei, L. Hao, N. Fang, M.W. Chang, R. Xu, Y. Yang, Y. Chen, Sharper and faster "nano darts" kill more bacteria: A study of antibacterial activity of individually dispersed pristine single-walled carbon nanotube, ACS Nano 3 (2009) 3891–3902.
[42] L. Shi, D.C. Shi, M.U. Nollert, D.E. Resasco, A. Striolo, Single-walled carbon nanotubes do not pierce aqueous phospholipid bilayers at low salt concentration, J. Phys. Chem. B 117 (2013) 6749–6758.